J Comput Aided Mol Des (2012) 26:437–450
DOI 10.1007/s10822-012-9572-z

# Structure-based design of oxygen-linked macrocyclic kinase inhibitors: discovery of SB1518 and SB1578, potent inhibitors of Janus kinase 2 (JAK2) and Fms-like tyrosine kinase-3 (FLT3)

**Anders Poulsen · Anthony William · Stéphanie Blanchard · Angeline Lee · Harish Nagaraj · Haishan Wang · Eeling Teo · Evelyn Tan · Kee Chuan Goh · Brian Dymock**

Received: 1 December 2011 / Accepted: 11 April 2012 / Published online: 22 April 2012


**Abstract** Macrocycles from our Aurora project were screened in a kinase panel and were found to be active on other kinase targets, mainly JAKs, FLT3 and CDKs. Subsequently these compounds became leads in our JAK2 project. Macrocycles with a basic nitrogen in the linker form a salt bridge with Asp86 in CDK2 and Asp698 in FLT3. This residue is conserved in most CDKs resulting in potent pan CDK inhibition. One of the main project objectives was to achieve JAK2 potency with 100-fold selectivity against CDKs. Macrocycles with an ether linker have potent JAK2 activity with the ether oxygen forming a hydrogen bond to Ser936. A hydrogen bond to the equivalent residues of JAK3 and most CDKs cannot be formed resulting in good selectivity for JAK2 over JAK3 and CDKs. Further optimization of the macrocyclic linker and side chain increased JAK2 and FLT3 activity as well as improving DMPK properties. The selective JAK2/FLT3 inhibitor **11** (Pacritinib, SB1518) has successfully finished phase 2 clinical trials for myelofibrosis and lymphoma. Another selective JAK2/FLT3 inhibitor, **33** (SB1578), has entered phase 1 clinical development for the non-oncology indication rheumatoid arthritis.

**Keywords** JAK2 · FLT3 · Inhibitor · Structure-based design · Docking · Subtype selectivity

A. Poulsen (✉) · A. William · S. Blanchard · A. Lee · H. Nagaraj · H. Wang · E. Teo · E. Tan · K. C. Goh · B. Dymock
S*BIO Pte Ltd, 1 Science Park Road, #05-09 The Capricorn, Singapore Science Park II, Singapore 117 528, Singapore
e-mail: anders@colours.dk

## Introduction

The Janus kinases (JAK) are a family of cytoplasmic tyrosine kinases consisting of JAK1, JAK2, JAK3 and TYK2. They play a pivotal role in the signaling pathways of numerous cytokines, hormones and growth factors [1]. Their intracellular substrates include the family of proteins called Signal Transducer and Activator of Transcription (STAT). The JAK-STAT pathways, through the proper actions of their cognate ligands, regulate important physiological processes such as immune responses, hematopoiesis, lactation, lipid homeostasis, etc. However, dysfunctional signaling caused by a myriad of factors results in pathological conditions such as allergies, asthma, rheumatoid arthritis, severe combined immune deficiency, hematological malignancies, etc. In particular, mutations in JAK2 have been associated with myeloproliferative disorders (including polycythemia vera, essential thrombocythemia and myelofibrosis) and a wide range of leukemias and lymphomas [2].

JAK2 was discovered in 1992 and found to be a ubiquitously expressed non-receptor tyrosine kinase [3]. Indications that hematological malignancies may arise from genetic alterations in JAK2 were first reported in 1997 [4]. Since then, 11 different genetic alterations including, substitutions, deletions and insertions have been detected. JAK2 substitutions, predominantly V617F and less frequently at other residues coded by exon 12, have been identified in almost all patients with polycythemia vera (PV) and approximately half of the patients with essential thrombocythemia (ET) and primary myelofibrosis (PMF) [5]. These gain-of-function mutations result in constitutive activation of JAK2 tyrosine kinase. Results from several case studies also suggest that the JAK2 mutation may be correlated with a poorer prognosis in patients with myeloproliferative diseases (MPD) [6–8]. Preliminary data

from clinical trials with JAK2 inhibitors have shown promising activity in MPD patients [9–12]. Importantly, the myeloproliferative disorders belong to an area of unmet medical need where treatment modalities have not been updated over the past few decades [13].

In a previous high throughput screen against Aurora A, a number of potent aminopyrimidine inhibitors were discovered. To achieve novelty an aminopyrimidine macrocycle was proposed and a number of these were synthesized. A screen against a kinase panel showed these macrocycles to be active against a small group of kinases, including CDK2, JAK2 and FLT3. Macrocycles bearing a basic centre in the linker ('nitrogen linked') inhibited JAK2 potently but were found to be low nanomolar cell cycle inhibitors [14]. 'Oxygen linked' macrocycles, discussed herein, were found to have a more attractive selectivity profile with potent FLT3 and JAK2 inhibition and low inhibitory activity against CDK2, hence consequently they became leads in our JAK2/FLT3 optimisation program. This paper discusses the structure-based design and explanations for the observed SAR using computational docking which ultimately led to the clinical candidates **11** (Pacritinib, SB1518) and **33** (SB1578).

## Computational methods

### Conformational search, force fields and solvation model

The molecules were built using Maestro 8.5.207 [15] or converted to 3D structures from the 2D structure using LigPrep version 2.5.207 [15]. Basic amines were protonated as in aqueous solution at physiological pH. The conformational space was searched using the Monte Carlo multiple minima (MCMM) method for torsional sampling [16] as implemented in MacroModel version 9.6.207 [15]. All heavy atoms and hydrogens on heteroatoms were included in the test for duplicate conformations. All rotatable single bonds were included in the conformational search and all aliphatic rings were ring-opened and quaternary atoms were allowed to invert. Each search was continued until the global energy minima were found at least 3 times. The energy minimizations were carried out using the truncated Newton conjugate gradient algorithm (TNCG) and the OPLS-2005 force field [17, 18] as implemented in MacroModel. The convergence was set to gradient with a threshold of 0.05 and maximum iterations to 500. The conformational searches were done for aqueous solution using the generalized Born/solvent accessible surface (GB/SA) continuum solvation model [19]. A constant dielectric of 1.0 was used with extended cutoff for van der Waals interactions of 8.0 Å, electrostatic interactions of 20 Å and hydrogen bonds of 4 Å.

### Docking

The JAK1 (PDB entry 1YVJ [20]), JAK2 (PDB entry 2B7A [21]), JAK3 (PDB entry 1YVJ [22]), TYK2 (PDB entry 3LXP [23]), CDK2 (PDB entry 1AQ1 [24]) and FLT3 (PDB entry 1RJB [25]) X-ray structures were downloaded from the protein data bank (http://www.pdb.org [26]). During the lead optimization program the JAK1 and TYK2 homology models (vide infra) were used where as the later released JAK1 and TYK2 X-ray structure were used for illustrations in this paper. The JAK2, JAK3 and FLT3 entries were the only structures published for these proteins at the start of the lead optimization program. The protein structures were prepared using the protein preparation wizard in Maestro. Bond orders were assigned, hydrogens added and waters deleted. Hydrogen bonds were assigned using exhaustive sampling of hydrogen bonds at neutral pH. Finally the structure were minimized with Impref using OPLS-2005 with a convergence on heavy atoms of 0.3 Å. Grids were generated using Glide version 5.0.207 [15] following the standard procedure recommended by Schrödinger. The bindingsite was defined by the ligand and van der Waals radii were not scaled on the receptor. A hydrogen bond constraint was included in the grid files. This is the hydrogen bond donor in the hinge region of the kinase to which the 1 position of the purine of ATP forms a hydrogen bond. The compounds were docked using Glide in standard precision mode with the settings "Sample nitrogen inversions", "Sample ring conformations", "Penalize nonplanar conformations of amide bonds" and a scaling factor for van der Waals radii of 0.8 with partial charge cutoff set to 0.15. As Glide is unable to treat macrocyclic rings flexibly, a conformational search was performed on each compound as previously described. The conformational ensemble was docked flexibly, i.e. only sidechains were treated flexibly by Glide. The docked poses discussed in this paper were not necessarily the highest scoring, but were selected as the highest scoring pose with a reasonable conformation and binding mode as judged by the modeler.

To evaluate the performance of the docking program and scoring function on the 2-aminophenyl-4-phenylpyrimidine scaffold the PDB was searched for kinase structures co-crystalized with small molecules having this scaffold. The CDK2 structure 2C5Y has a 2-aminophenyl-4-phenylpyrimidine ligand with both phenyls meta substituted and the substituents are pointing towards each other. The structure was prepared and the ligand docked in both the SP and XP mode. The RMSD between the co-crystalized ligand and the closest docked pose was 0.44 Å for the highest scoring pose for Glide SP and 0.24 Å for the second highest scoring pose for Glide XP.

## Homology and protein modeling

Homology models were build for JAK1 and TYK2. The protein sequences for JAK1 (accession number P23458) and TYK2 (accession number P29597) were downloaded from uniprot (http://uniprot.org [27]). The kinase domains were aligned to those of JAK2 & JAK3 using clustal W 1.83 [28] and then manually edited. The sequence identity is 51–62 % and homology is 70–78 % Secondary structure was taken from the X-ray structures and predicted by Psipred [29] and SSPro [30] for JAK1 and TYK2. The alignment and structure prediction is shown in Fig. 1. The JAK2 X-ray structure was used as template. The homology models were built using Prime 2.0.208 [15] with the settings "Retain rotamers for conserved residues", "Minimize residues not derived from template" and "Include ligands". Loops were not optimized, as we were only interested in the ATP-binding site, which is well conserved in the JAK family. The homology models were finally subjected to 5000 steps of Steepest Decent minimization using MacroModel [15] with OPLS-2005 force field [18] and the GB/SA solvation model [31]. The FLT3 and FGFR2 (PDB entry 1OEC) X-ray structures were downloaded from the protein data bank (PDB). The FLT3 X-ray structure is in the DFG-out conformation, which prevents our inhibitors from being docked into the ATP binding site. A search of the PDB revealed that FGFR2 is the kinase with the highest homology to FLT3 for which a DFG-in conformation is available. The FGFR2 X-ray structure was superimposed on FLT3 using the structure alignment tool in Maestro. Residues Asp829-Pro851 of FLT3 was manually modeled after the corresponding residues in the FGFR2 structure. The FLT3 model was subjected to 5000 steps of Steepest Decent minimization using OPLS-2005 and GB/SA. The resulting hybrid X-ray/homology model FLT3 structure was prepared for docking as previously described.

## Calculation of the conformational energy penalty

The docked conformation was minimized with MacroModel using flat bottom Cartesian constraint with a half width of 1.0 Å and the default restraining force constant of 100 kJ/mol. This allows the docked conformations to relax (adjust) to the OPLS-2005 force field. Without the relaxation the energy calculated by OPLS-2005 would be meaningless. This relaxation does not change the conformation as RMS between the docked and relaxed structures are <0.1 Å. The conformational energy penalty of the docked conformations was calculated by subtracting the internal (steric) energy of the preferred conformation in aqueous solution (i.e. the energy of the global energy minimum in solution excluding the hydration energy) from the calculated energy of the docked conformation. Since the conformational ensemble was represented by only the global energy minima, entropy effects have not been taken into account. For flexible molecules this leads to an underestimation of the energy penalty. A limit of 3 kcal/mol (12.6 kJ/mol) for acceptable energy penalties was imposed as recommended by Boström et al. [32].

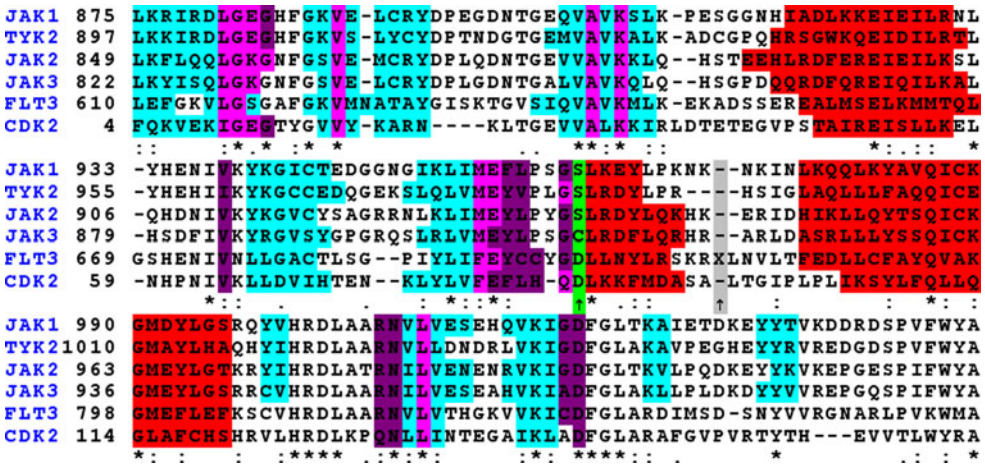


**Fig. 1** Clustal W alignment of the studied protein kinases. *Cyan*: beta sheet; *red*: alpha helix; *purple*: binding site; *magenta*: binding site and beta sheet. Secondary structure information is taken from the X-ray structures. The protein structures were aligned using the Maestro structure alignment tool and the binding site residues were determined as those within 4 Å of all co-crystallized ligands. The *X highlighted in grey* denotes the FLT3 insertion residues 708–779. The *arrow highlighted with green* indicates a residue essential for the selectivity of the described macrocycles

### Calculation of ligand protein interaction energies

Residues further from the ligand than 7 Å was constrained. The ligand protein complex was minimized using MacroModel and 50 steps of TNCG minimization. The absolute energy of the ligand–protein complex was calculated by MacroModel using current energy with water as a solvent, dielectric constant of 1 and extended cutoffs. The absolute energy of the isolated protein and ligand was substracted.

### Calculation of physical properties

The 2D structures were converted to 3D using LigPrep with the -qik option. This option neutralizes the output structures as appropriate for QikProp input. Physical properties except $pK_a$ values were calculated using QikProp version 3.1.207 [15] in standard mode. pKa values were calculated with Epik version 1.6.207 [15]. Solvent was set to water with a pH of 7.0 ± 2.

### DFT calculations

The program Jaguar version 7.5.207 [15] was used for Hybrid B3LYP DFT energy minimization with a convergence criteria of 5*10-5 hartree. The chosen basis set was 6-31G**. The PBF solvation model [33] was used with water as solvent, a dielectric constant of 80.37 and a density of 0.99823 g/mL. Accuracy level was set to "Accurate" and grid density was set to "Fine".

### In vitro kinase assays

These recombinant kinases were generated by the Protein Biochemistry Group in S*BIO: CDK2/CyclinA, FLT3, JAK1, JAK2, JAK3 and TYK2. All assays were carried out in 384-well white microtiter plates using the PKLight assay system from Cambrex. This assay platform is essentially a luminometric assay for the detection of ATP in the reaction using a luciferase-coupled reaction. The analytical software Prism 4.0 [34] was used to generate $IC_{50}$ values from the data.

For CDK2/Cyclin A assay, the reaction mixture consisted of the following components in 25 µL assay buffer (50 mM Hepes pH 7.5, 10 mM $MgCl_2$, 5 mM $MnCl_2$, 5 mM beta-glycerophosphate, 1 mM dithiothreitol, 0.1 mM sodium orthovanadate), 1.4 µg/mL of CDK2/Cyclin A complex, 0.5 µM of RbING substrate (Invitrogen, Cat # PV2939) and 0.5 µM of ATP. The compounds were tested at 8 concentrations prepared from fourfold serial dilution starting at 10 µM. The reaction was incubated at room temperature for 2 h. 13 µL of PKLight ATP detection reagent was added and the reaction was incubated for 10 min. Luminescence signals were detected on a multilabel plate reader (Victor$^2$ V 1420, Perkin-Elmer).

The other kinase assays were constituted and performed in a similar manner except for the following differences in reagents:

For FLT3 assays, the reaction contained 1.3 µg/mL FLT3 enzyme, 5 µM of poly(Glu,Tyr) substrate (Sigma, Cat # P0275) and 0.15 µM of ATP.
For JAK1 assays, the reaction contained 2.5 µg/mL of JAK1 enzyme, 10 µM of poly(Glu,Ala,Tyr) substrate (Sigma, Cat # P3899) and 0.25 µM of ATP.
For JAK2 assays, the reaction contained 0.35 µg/mL of JAK2 enzyme, 10 µM of poly(Glu,Ala,Tyr) substrate (Sigma, Cat # P3899) and 0.15 µM of ATP.
For JAK3 assays, the reaction contained 1.0 µg/mL of JAK3 enzyme, 10 µM of poly(Glu,Ala,Tyr) substrate (Sigma, Cat # P3899) and 1.5 µM of ATP.
For TYK2 assays, the reaction contained 2.5 µg/mL of TYK2 enzyme, 10 µM of poly(Glu,Ala,Tyr) substrate (Sigma, Cat # P3899) and 0.15 µM of ATP.

## Results and discussion

### Binding-mode and selectivity analysis

Development of CDK active macrocycles, which are nitrogen linked, like compound **1** (Fig. 2), have been reported elsewhere [14]. Figure 3 display a pose of **1** docked into JAK2. The aromatic rings are sandwiched between the hydrophobic residues Leu855, Val863 and Ala880 on the C-terminal side of the binding pocket and Leu983 and Val911 on the N-terminal side. The aromatic rings have hydrophobic contacts to the sidechain of the gatekeeper residue Met929, Leu932 in the hinge region and the alpha carbon of Gly935. The aminopyrimidine moiety forms two hydrogen bonds to Leu932 in the kinase hinge region. An additional hydrogen bond is formed between the basic nitrogen of the macrocyclic linker and the hydroxyl group of Ser936. 2-aminophenyl-4-phenylpyrimidines are known from X-ray structures like 2C5Y and 1OEC to bind to the active conformation of protein kinases with the described binding mode. The cyclization of the 2-aminophenyl-4-phenylpyrimidine scaffold prevents the compounds from adopting an extended conformation found in X-ray structures of compounds binding to the inactive conformation of tyrosine kinases like in 3GVU. The nitrogen linked macrocycles were found to be broadly acting kinase inhibitors when they were screened against a kinase panel, e.g. **1** is both a pan-JAK and pan-CDK inhibitor (Table 1). In order to explore selectivity, macrocycles with oxygen linkers such as compound **2** were

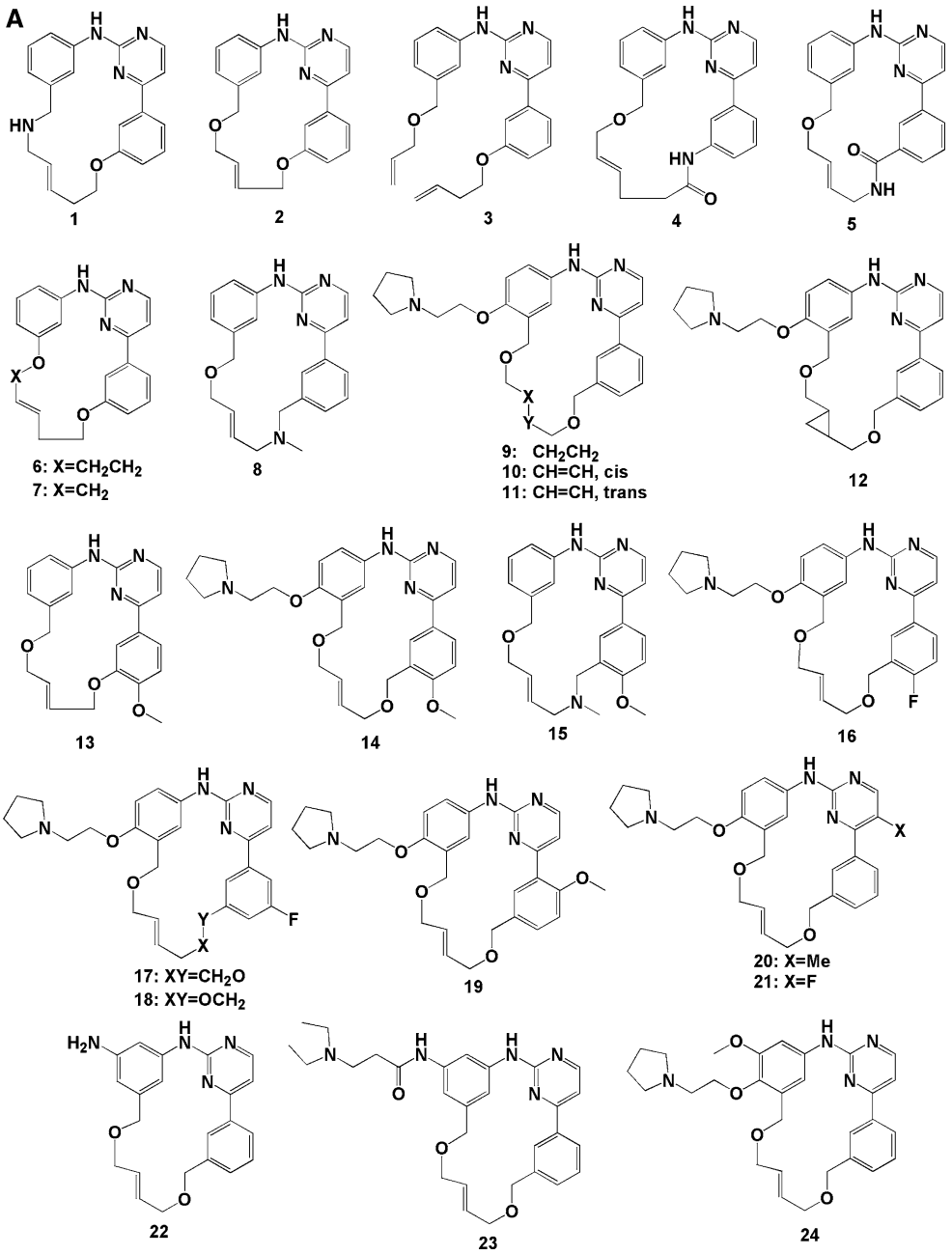


**Fig. 2** Biological data can be found in Table 1. Compounds **1–2** were leads originally designed to be Aurora inhibitors. The remaining macrocycles were synthesized for the JAK2 project

synthesized and tested. These were found to be more selective than the nitrogen linked isomers. Figure 4 show the putative binding mode of **2** docked into JAK2. Compound **2** binds to JAK2 in a similar fashion to **1** but it makes a hydrogen bond to Ser936, whereas **1** has a basic nitrogen in the linker, which can act as both a hydrogen bond donor and acceptor as well as forming salt bridges to acidic residues. Compound **2** has an ether oxygen that may only hydrogen bond to residues that contain hydrogen bond donors. Figure 1 displays a clustal-W alignment of the JAK family as well as CDK2 and FLT3. The arrow highlighted in green marks Ser936 in JAK2 and its homologous residues. JAK1, JAK2 and TYK2 are the only kinases in the alignment with a residue having a sidechain with a hydrogen bond donor in this position. JAK3 has a cysteine residue in this position, which is expected to make weaker hydrophobic interactions with the macrocyclic linker of **2**. On the other hand, CDK2 and FLT3 have an acidic aspartate at this position which would be expected to interact repulsively with the ether oxygen of the macrocyclic linker. Compound **2** has reduced CDK2 activity compared to **1**, but surprisingly not reduced FLT3 activity. When **2** is docked into FLT3 (Fig. 5, left) the putative binding mode is similar to JAK2. However instead of the

**Fig. 2** continued

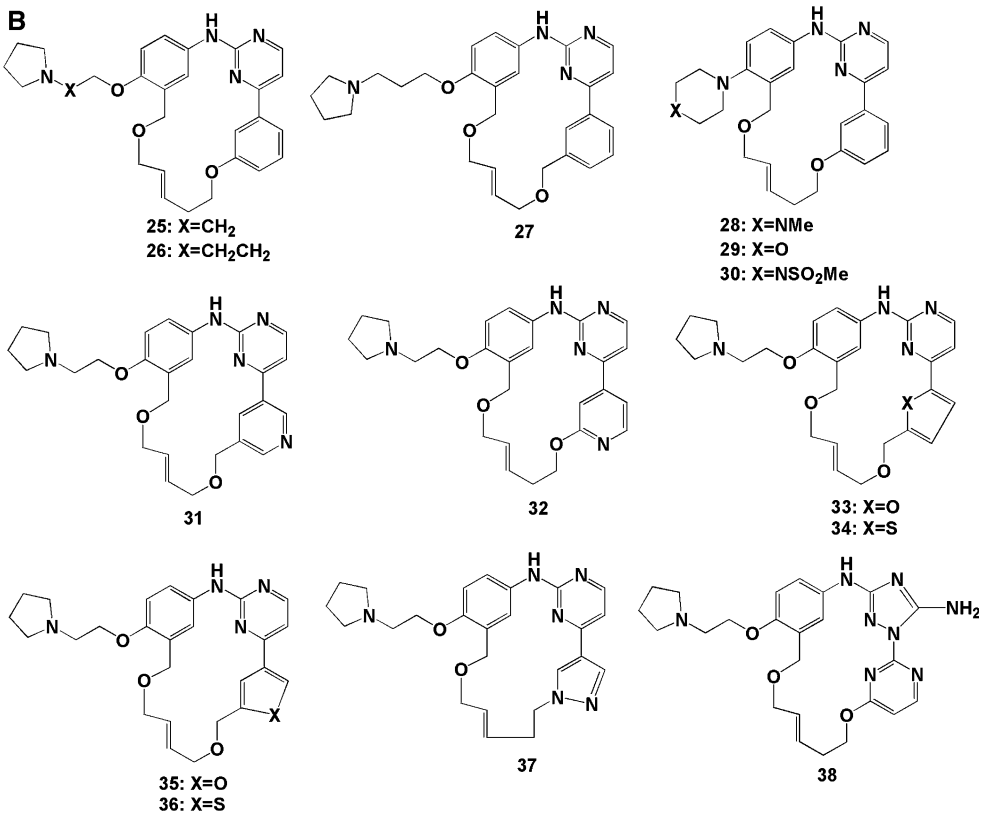


hydrogen bond between the ether oxygen and Ser936 a hydrogen bond to the backbone nitrogen of Asp698 is observed. The putative CDK2 binding mode of **2** is shown in Fig. 5, right. The ether oxygen is unable to interact with the backbone nitrogen of the equivalent residue Asp86. The sequence alignment in Fig. 1 shows that in CDK2 there is a one residue deletion between the hinge region and Asp86. Therefore the backbone nitrogen of Asp86 is closer to the hinge region than Asp698 in FLT3 and it is not possible for the ether oxygen of **2** to hydrogen bond to the backbone of Asp86 in CDK2. To evaluate the importance of the electrostatic interaction between the ether oxygen and residue 86 of CDK2, the interaction energy of the ligand–protein complex of **2** was calculated. Asp86 was then mutated to a serine which was modeled to form a hydrogen bond of 2.8 Å to the ether oxygen but this complex was not minimized. The interaction energy between **2** and Ser86 mutated CDK2 was calculated. The difference in interaction energies was found to be 11.7 kJ/mol more favorable in the mutated complex. This hypothetical difference corresponds to a difference in binding constants of 110 fold. We attribute the reduced CDK2 activity of **2** to the observation that a hydrogen bond to Asp86 cannot be formed.

These findings explain the relative activity of oxygen linked macrocycles towards CDK, FLT3, JAK2, JAK3 and TYK2 kinases (Table 1). JAK1 also has a serine in the equivalent position of Ser936 in JAK2 hence the complete lack of JAK1 activity of the oxygen linked inhibitors were therefore a surprise. The binding sites of JAK1 and JAK2 are very similar geometrically and all residues involved in binding of the macrocycles are conserved. However the hydrogen bonding network around Ser936 and the equivalent JAK1 residue Ser963 are different as illustrated in Fig. 6. The protein structures in Fig. 6 were prepared as described (vide supra) except for the minimization step, which was excluded. In JAK2, the hydroxyl group of Ser936 does not hydrogen bond to any residues in the protein, and therefore Ser936 is free to form a hydrogen bond to the linker oxygen of the macrocycles. In JAK1, the hydroxyl group of Ser963 hydrogen bonds to Glu966 and Lys965. Therefore Ser963 is not free to hydrogen bond to oxygen linked inhibitors. However the hydroxyl is free to act as a hydrogen bond acceptor, suggesting an explaination for the JAK1 activity of compound **1**, a nitrogen linked macrocycle.

## Selection of linker

With the realization that the macrocycles interacted with a residue that could be exploited to make selective JAK2/FLT3 inhibitors, it was decided to embark on an optimisation program with the aim of making oxygen-linked macrocycles with potency for JAK2 and FLT3 and >100-fold selectivity for CDK2. Figure 7 shows the markush

**Table 1** Biological data for the compounds shown in Fig. 2

| Compound | JAK1 IC50 | JAK2 IC50 | JAK3 IC50 | TYK2 IC50 | CDK2 IC50 | FLT3 IC50 | Solubility |
|---|---|---|---|---|---|---|---|
| **1 (Lead)** | 0.18 ± 0.021 | 0.15 ± 0.083 | NA | 0.081 ± 0.005 | 0.021 ± 0.012 | 0.11 ± 0.038 | 15 |
| **2 (Lead)** | >10 | 0.28 ± 0.035 | NA | 0.63 ± 0.063 | 0.11 ± 0.014 | 0.10 ± 0.001 | NA |
| **3** | NA | 5.5 ± 0.78 | NA | NA | >10 | 3.7 ± 0.35 | NA |
| **4** | >10 | 5.3 ± 0.42 | >10 | >10 | 1.6 ± 0.21 | >10 | NA |
| **5** | >10 | 0.20 ± 0.0071 | NA | 0.78 ± 0.063 | >10 | 2.1 ± 0.71 | NA |
| **6** | >10 | 1.2 ± 0.66 | >10 | 5.2 ± 0.50 | >10 | 1.1 ± 0.49 | NA |
| **7** | >10 | 0.23 ± 0.014 | >10 | 0.070 ± 0.0085 | 0.33 ± 0.16 | 0.088 ± 0.013 | NA |
| **8** | 3.2 ± 0.92 | 0.23 ± 0.0071 | NA | 0.83 ± 0.078 | 0.099 ± 0.016 | 0.31 ± 0.035 | NA |
| **9** | 1.1 ± 0.61 | 0.076 ± 0.024 | 1.6 ± 0.51 | 0.11 ± 0.023 | 1.3 ± 0.64 | 0.027 ± 0.0079 | NA |
| **10** | 2.2 ± 0.46 | 0.065 ± 0.016 | 1.1 ± 0.71 | 0.23 ± 0.0071 | 3.9 ± 0.66 | 0.080 ± 0.02 | NA |
| **11 (SB1518)** | 1.28 ± 0.37 | 0.023 ± 0.006 | 0.52 ± 0.11 | 0.050 ± 0.006 | 3.9 ± 1.07 | 0.022 ± 0.006 | 150 |
| **12** | 2.8 ± 0.071 | 0.073 ± 0.02 | 0.57 ± 0.063 | 0.22 ± 0.042 | 3.5 ± 0.85 | 0.037 ± 0.0097 | NA |
| **13** | >10 | 0.096 ± 0.0042 | NA | 0.33 ± 0.05 | 5.0 ± 1.7 | 0.039 ± 0.0035 | NA |
| **14** | >10 | 0.019 ± 0.0021 | 0.89 ± 0.042 | 0.18 ± 0.0 | >10 | 0.092 ± 0.011 | 61 |
| **15** | >10 | 0.69 ± 0.028 | NA | 1.4 ± 0.28 | >10 | 0.41 ± 0.0071 | NA |
| **16** | 4.6 ± 0.35 | 0.025 ± 0.0014 | 0.72 ± 0.11 | NA | 3.3 ± 0.071 | 0.040 ± 0.015 | NA |
| **17** | 0.38 ± 0.014 | 0.024 ± 0.0021 | 0.50 ± 0.028 | 0.036 ± 0.0028 | 2.0 ± 0.42 | 0.0077 ± 0.00035 | NA |
| **18** | 1.2 ± 0.26 | 0.039 ± 0.0014 | 0.95 ± 0.028 | 0.058 ± 0.005 | 1.3 ± 0.42 | 0.10 ± 0.0092 | 2.6 |
| **19** | 4.9 ± 0.85 | 0.33 ± 0.0 | 7.2 ± 0.21 | 0.62 ± 0.064 | >10 | 0.012 ± 0.00071 | NA |
| **20** | 1.0 ± 0.0 | 0.0066 ± 0.00042 | 0.089 ± 0.0035 | 0.057 ± 0.0042 | >10 | 0.019 ± 0.0014 | 178 |
| **21** | 0.83 ± 0.085 | 0.017 ± 0.0 | 1.0 ± 0.0 | 0.14 ± 0.028 | 1.6 ± 0.071 | 0.015 ± 0.0028 | NA |
| **22** | NA | 0.035 ± 0.00071 | 1.75 ± 0.071 | NA | 0.24 ± 0.028 | 0.052 ± 0.028 | 25 |
| **23** | 1.9 ± 0.21 | 0.044 ± 0.0035 | 0.39 ± 0.15 | 0.018 ± 0.005 | 0.4 ± 0.11 | 0.078 ± 0.0071 | NA |
| **24** | 1.7 ± 0.28 | 0.036 ± 0.0028 | 1.75 ± 0.071 | 0.17 ± 0.021 | 3.4 ± 1.1 | 0.0064 ± 0.0013 | 154 |
| **25** | 1.7 ± 0.21 | 0.051 ± 0.012 | 0.90 ± 0.14 | 0.1 ± 0.014 | 6.9 ± 2.6 | 0.12 ± 0.046 | NA |
| **26** | 1.2 ± 0.0 | 0.021 ± 0.0071 | 0.59 ± 0.33 | 0.059 ± 0.005 | 4.5 ± 1.8 | 0.030 ± 0.0042 | NA |
| **27** | 1.6 ± 0.14 | 0.019 ± 0.0014 | 0.43 ± 0.0071 | 0.063 ± 0.0085 | >10 | 0.037 ± 0.02 | NA |
| **28** | 3.6 ± 0.41 | 0.041 ± 0.0051 | 1.6 ± 0.096 | 0.19 ± 0.026 | 7.7 ± 0.0 | 0.030 ± 0.0071 | 26 |
| **29** | 8.7 ± 1.06 | 0.06 ± 0.0014 | >10 | 0.16 ± 0.014 | >10 | 0.032 ± 0.012 | NA |
| **30** | >10 | 0.15 ± 0.021 | >10 | 0.14 ± 0.035 | >10 | 0.15 ± 0.028 | NA |
| **31** | >10 | 0.29 ± 0.085 | 1.0 ± 0.13 | 0.63 ± 0.028 | 3.2 ± 0.14 | 0.063 ± 0.0028 | NA |
| **32** | 0.97 ± 0.26 | 0.018 ± 0.0027 | 1.4 ± 0.18 | 0.030 ± 0.003 | 0.27 ± 0.059 | 0.031 ± 0.0062 | NA |
| **33 (SB1578)** | 2.7 ± 0.81 | 0.046 ± 0.0069 | 4.3 ± 1.8 | 0.23 ± 0.046 | 6.7 ± 1.8 | 0.060 ± 0.013 | >250 |
| **34** | 0.42 ± 0.12 | 0.0073 ± 0.0016 | 0.65 ± 0.17 | 0.032 ± 0.0085 | 2.9 ± 0.81 | 0.024 ± 0.0061 | 154 |
| **35** | 3.0 ± 0.49 | 0.067 ± 0.0071 | 8.8 ± 0.57 | 0.12 ± 0.0071 | >10 | 0.048 ± 0.014 | >250 |
| **36** | 1.5 ± 0.14 | 0.017 ± 0.0035 | 0.68 ± 0.17 | 0.047 ± 0.0 | 6.8 ± 0.35 | 0.045 ± 0.018 | 218 |
| **37** | 4.2 ± 0.14 | 0.12 ± 0.014 | 1.6 ± 0.14 | 0.13 ± 0.0071 | 0.54 ± 0.071 | 0.032 ± 0.0042 | NA |
| **38** | >10 | 0.27 ± 0.023 | 4.5 ± 0.64 | 0.67 ± 0.076 | >10 | 0.023 ± 0.0014 | NA |

The $IC_{50}$ values and standard deviations are in micromolar. The $IC_{50}$ values are the mean of at least two individual determinations. High throughput solubility in PBS buffered at pH 7.0 is in μg/mL

*NA* data not available

structure of oxygen linked compounds compatible with our ring closing methathesis synthetic route and proposed binding mode. The 324 possible macrocycles (i.e. m*n*o*p*Y = 3*3*3*3*4) were built and a conformational search was performed on each compound. The resulting conformer ensembles were docked into JAK2. The linkers that docked best were those with m = 0–2, n = 1, o = 1–2, p = 0–1 and Y = O, NHCO and NH. To find the optimal linker, a number of the best binders were synthesized.

Compound **3**, a substrate for ring closure methathesis, indicates that the macrocyclic ring closure is important for activity. The sidechains of **3** have many degrees of freedom and are expected to have a higher entropy penalty upon

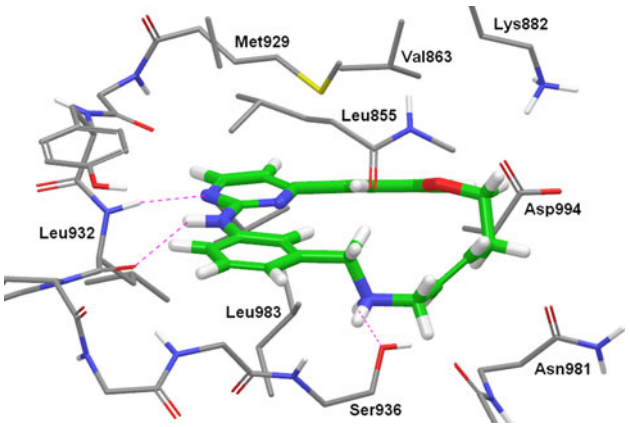


**Fig. 3** Compound **1** (thick tube representation with *green* carbon atoms) docked into the JAK2 ATP-binding site that is shown in *thin tube* with *grey* carbon atoms. Hydrogen bonds are shown in *magenta dashed lines*. The aminopyrimidine of **1** forms two hydrogen bonds to the backbone of Leu932 and the basic nitrogen forms a hydrogen bond with the hydroxyl group of Ser936

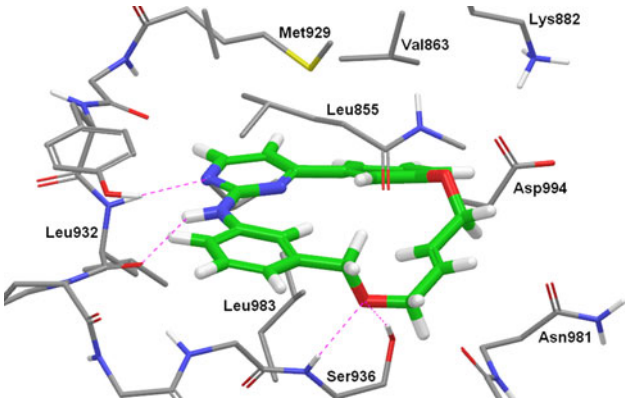


**Fig. 4** Compound **2** docked into the JAK2 ATP-binding site. The ether oxygen of **2** forms a hydrogen bond with the hydroxyl group of Ser936

binding than its ring closure product. Compound **3** were found to have 673 conformations below 21 kJ/mol compared to 162 for **1**. However the macrocyclic linker may also lock the aromatic ring system into low energy conformations that are not accessible to analogues that are not macrocycles. Determining the linker that gives the best fit of a low energy conformation to the JAK2 binding site depends crucially on the length and rigidity of the linker.

Amide **4** was docked into the JAK2 binding site. All poses that formed a hydrogen bond to Ser936 had the amide oxygen pointing towards oxygen atoms in the sidechains of Asn981 and Asp994 or the backbone of Arg980. The shortest distance from the amide oxygen of **4** to a protein oxygen were between 2.8 and 3.1 Å. These repulsive interactions are consistent with the reduced activity. In contrast, for compound **5**, all poses with a hydrogen bond to Ser936 had the amide hydrogen bond donor pointing towards the sidechains of Asn981 and Asp994 consistent with a 25 fold increased JAK2 activity compared to **4**.

Due to the shorter distance between the B-ring and the linker heteroatom, compounds with a phenolic linker attached to the B-ring may hydrogen bond with both the backbone NH and sidechain of Ser936, whereas benzylic linkers may only hydrogen bond with the sidechain of Ser936. Compound **6** has the same ring size as **1**, but the benzylic basic amine has been exchanged for a phenolic oxygen. When docked, low energy conformations of **6** formed hydrogen bonds to the backbone NH of Ser936, the sidechain of Ser936 or both. However in these poses the methylene groups between the B-ring and the double bond clashed with the glycine rich loop and/or Ser936. Compound **7** has one methylene group less between the B-ring and the double bond. Low energy conformations of **7** hydrogen bonded with Ser 936 but the methylene did not

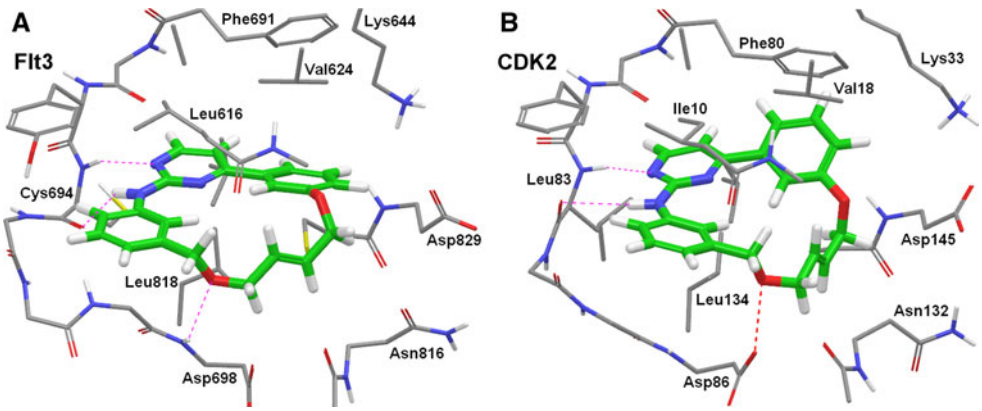


**Fig. 5** **a** Compound **2** docked into FLT3. Similar hydrophobic interactions and hydrogen bonds to the hinge region are observed as for JAK2. However the ether oxygen forms a hydrogen bond to the backbone NH donor of Asp698. **b** Compound **2** docked into CDK2. The ether oxygen does not hydrogen bond to any CDK2 residues. However it is within hydrogen bonding distance of Asp86. This is an unfavorable interaction that can explain the order of magnitude reduction in CDK activity of oxygen linked macrocycles as compared to the N-linked compound **1**

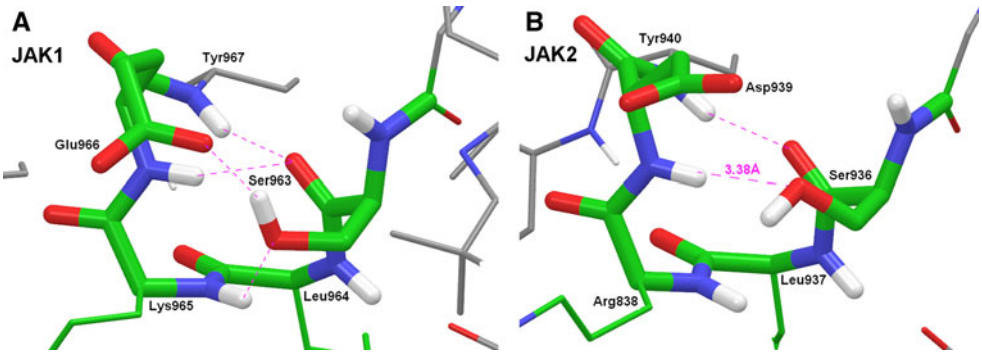


**Fig. 6** **a** In JAK1, the hydroxyl group of Ser963 hydrogen bonds to Glu966 and Lys965. Therefore Ser963 is not free to hydrogen bond to the inhibitor. **b** In JAK2, the hydroxyl group of Ser936 does not hydrogen bond to any residues in the protein, and therefore Ser936 is free to form a hydrogen bond to the linker oxygen of the macrocycles. Although the hydroxy of Ser936 points towards the backbone NH of Asp939 the distance between the groups is too long for a hydrogen bond

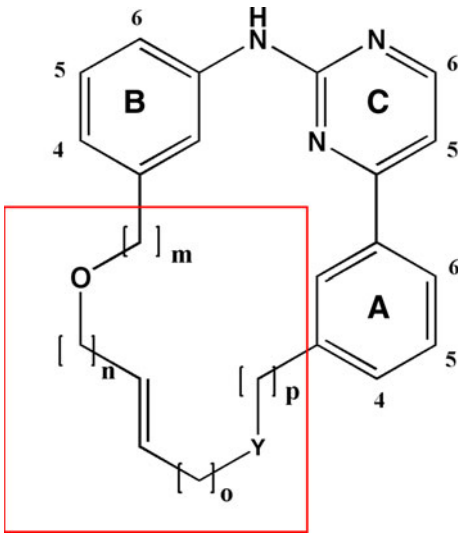


**Fig. 7** *Left* The structure of the proposed macrocycles. The 3 aromatic rings in the compounds discussed here will be referred to as the *A*, *B* or *C*-ring, respectively. The part of the macrocycle shown inside the *red box* will be referred to as the linker. Macrocycles compatible with our synthetic route and proposed binding-mode could have m, p = 0–2, n, o = 1–3 and Y = NR, O, CONH, NHCO

clash with the protein explaining the increased potency of **7** relative to **6**. However the increased CDK2 activity disqualified **7** as a lead.

The heteroatom between the A-ring and the double bond falls into a more hydrophilic area and the proximity of the heteroatom to Asp994 led us to introduce a basic nitrogen in this position. Compound **8** with a methyl group on the basic nitrogen docked well forming hydrogen bonds with the hinge as well as Ser936. However the methyl group of the basic nitrogen pointed towards Asp994 preventing any salt bridge formation. Conformations with the methyl pointing in other directions had the methyl clashing slightly with the protein. When docked into CDK2 the methyl may be accommodated without clashing with the protein and a salt bridge may form between Asp145 and the basic nitrogen. Compound **8** was found to be equipotent with **2** against JAK2 but it retained significant CDK2 activity. The high CDK2 activity of **8** and the SAR of nitrogen linked macrocycles [14] stopped us from making analogues of **8** without substituents on the basic nitrogen.

A symmetric 8-atom linker with benzylic oxygen resulted in compounds with good JAK2 activity and a favorable selectivity profile. Several low energy conformations docked well forming the previously discussed hydrogen bonds with a good geometry. Figure 8a shows a representative conformation of **11** docked into JAK2. Figure 8b shows good van der-Waal contacts between JAK2 and **11**. Notice that the macrocyclic ring, especially the benzylic methylenes, contribute favorably to binding. This macrocyclic ring was chosen for further optimization, and a few derivatives of the macrocyclic ring were synthesized. As these have low aqueous solubility all compounds with this scaffold were synthesized with a solubilising side chain unless they incorporated other solubilizing features (vide infra). Compound **9** with a saturated linker was threefold less potent than **11**. As twice the number of low energy conformations were found for **9**, an entropy penalty may account for at least part of the difference in binding energy. Compound **10** with a cis double bond was also 3 times less potent than **11**. When docked into JAK2 **10** had a lower docking score and fewer conformations could be docked than for **11**. The difference in activity may be due to a better shape fit of **11** to the binding site. Compound **12** with a cyclopropyl in place of the double bond docked well with a docking score comparable to that of **11**. However fewer conformations could be docked due to the larger size of the cyclopropyl and the JAK2 activity was found to be threefold less than that of **11**. Compounds **9**–**12** had the same selectivity profile and the trans isomer **11** docked better than the cis isomer **10** into all targets. Furthermore the trans isomer was the major

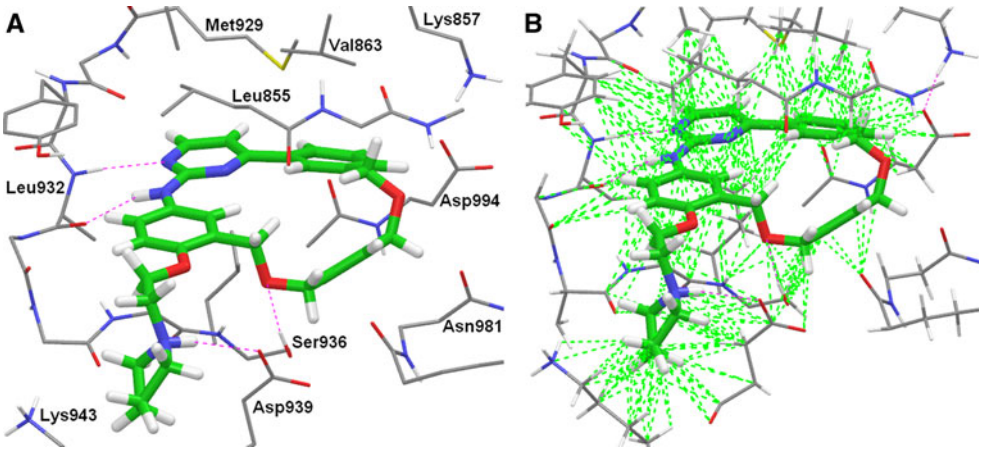


**Fig. 8** **a** Compound **11** (SB1518) docked into JAK2. The compound makes two hydrogen bonds to the hinge backbone and a hydrogen bond to the sidechain of Ser936. The basic nitrogen of the pyrrolidine side chain may form a salt bridge to Asp939. However Asp939 is a surface residue and the salt bridge may consequently be weak. **b** Favorable Van der-Waal contacts are shown as *green dashed lines* and hydrogen bonds as *magenta dashed lines*. The aromatic rings, the methylene groups of the macrocyclic linker and even the solubility tag have excellent hydrophobic interactions with the protein

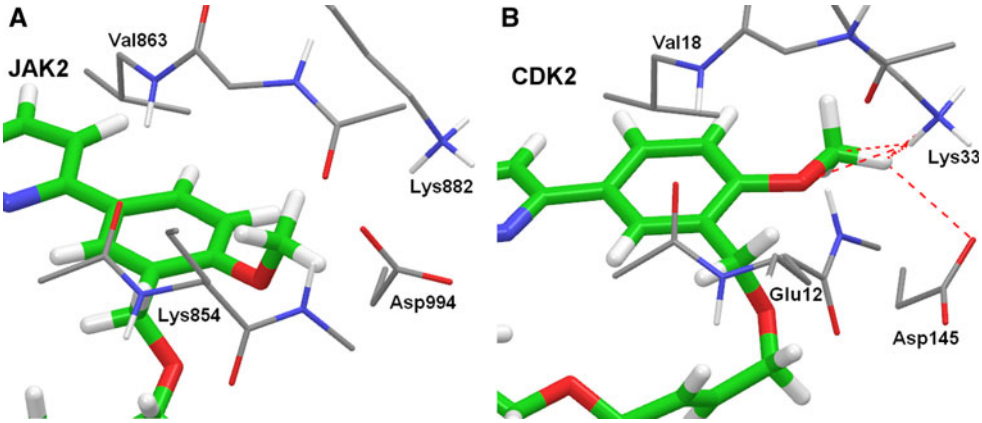


**Fig. 9** **a** Compound **14** docked into JAK2. The 4-methoxy substituent of the *A*-ring points up into the hydrophobic area between the sidechain of Val863, Lys882 and the backbone of Lys854. **b** The methoxy is in the same plane as the *A*-ring in the CDK2 pose making contact with the charged groups of Lys33 and Asp145

synthetic product hence optimization studies focused on this linker.

## Lead optimization for JAK2 subtype selectivity

Docking into JAK2 indicated that there is room for small substituents in the 4 and 5 position of the A-ring (see Fig. 7 for the numbering of the positions in the rings). We believed two atom groups such as methoxy were the maximum size of the substituent that could be accommodated in the JAK2 binding site. Hence a number of compounds with methoxy in the 4-position were made. The area in front and below the 4-position is rather polar with the sidechains of Asp994, Lys882 and Asn981 while the area above is hydrophobic surrounded by the backbone of Gly858 and Lys857 of the glycine rich loop, Val836 and methylenes of the sidechain of Lys882. The methoxy substituents of compounds **13**–**15** dock well into this hydrophobic area (Fig. 9a shows example **14**). DFT calculations show this out of plane conformation is up to 8 kJ/mol higher in energy than the in-plane conformation, but the conformational energy penalty may be offset by the extra hydrophobic interactions as the JAK2 activity is the same for compounds without the 4-methoxy (compare **13** with **2** and **14** with **11**). The addition of the methoxy made **14** more selective for JAK2 over CDK2 with a CDK2 $IC_{50}$ of greater than 10 μM compared to 3.9 μM for **11**. Figure 9b shows **14** docked into CDK2 with the methoxy in plane and clashing with the charged residues Lys33 and Asp145. In CDK2 the catalytic lysine Lys33 forms a salt bridge with Asp145. In order for the methoxy of **14** to point into the hydrophobic area above the aromatic ring system, Lys33 has to move away thereby disrupting the salt bridge. This may also be the reason for the decreased FLT3 activity while in FLT3 the catalytic lysine Lys644 may form a salt bridge to both Asp829 and Glu661. JAK1 activity was also decreased to more than 10 μM for **14** compared to 1.28 μM for **11**. Some conformations of **14**

could be docked into JAK1 with the methoxy out of plane pointing up into the hydrophobic area. However these were high energy conformations more than 12 kJ/mol above the global energy minima. Compound **15** is the methoxy derivative of **8** that had a reduced activity towards all kinases, particularly CDK2. This may be due to an internal hydrogen bond being formed between the basic nitrogen and the methoxy oxygen thereby increasing the conformational energy penalty of the bioactive conformation and, when bound to CDK2, preventing salt bridge formation to Asp145.

The fluorine analogue of **11**, compound **16**, was equipotent with **11** and of similar selectivity. This is in agreement with docking, as it seems the fluorine does not form any particular favorable or unfavorable interactions with the kinases.

The 5-position substituent of the A-ring is pointing towards the terminal of the gatekeeper with room for one heavy atom substituent, preferably hydrophobic. The slightly hydrophobic fluorine analogue, compound **17** is equipotent with **11** against JAK2 but less selective as it is threefold more potent on JAK1 and FLT3. The slightly less active **18** has the same selectivity profile with the exception of the FLT3 activity was reduced by an order of magnitude. Docking predicted that there is no room for substituents in the 6-position of the A-ring as the hydrogen in the 6-position has hydrophobic contact with the gatekeeper. Compound **19**, with a methoxy in the 6-position, is much less active, apart from FLT3. The docked poses of **19** are shifted out of the binding site compared to compounds without the 6-substituent.

For macrocycles docked into all JAK subtypes there is space for a small substituent in the 5 position of the C-ring. This position is pointing towards the central part of the sidechain of the gatekeeper, which is a methionine in all JAK kinases and a phenylalanine in FLT3 and CDK2. Interaction with these substituents is known to enhance affinity towards some protein kinases for non-macrocycles with the 2-aniline-4-phenyl-pyrimidine scaffold [35–37]. Compound **20**, with a methyl substituent, proved to be 3 times more potent on JAK2, equipotent on JAK1 and FLT3 and less than 10 μM on CDK2 when compared with **11**. However JAK3 activity also increased sixfold, which was detrimental to our target selectivity profile. Figure 10 shows **20** docked into JAK2. The addition of the methyl group increases the hydrophobic contacts with the gatekeeper. In CDK2 the C-ring has aromatic–aromatic interactions with the sidechain of the gatekeeper residue while this is not the case for FLT3 as the distance is too big (Fig. 5). The addition of the methyl presumably prevents the formation of the aromatic–aromatic interaction in CDK2. Compound **21** with the slightly smaller and less hydrophobic fluorine substituent had a similar activity profile to **11**.

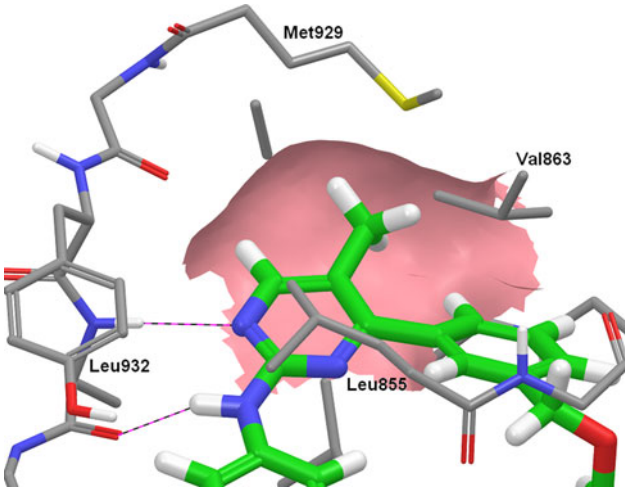


**Fig. 10** Compound **20** docked into JAK2. There is just enough room in the JAK2 binding site to accommodate the methyl group, which is a perfect shape fit to the binding site

## Lead optimization of ADME properties

Compound **1** had an aqueous solubility of 15 μg/mL while its N–Me analogue had a solubility of 72 μg/mL. While compounds incorporating a basic nitrogen in the macrocyclic linker like **1** were water soluble, the oxygen linked compounds had a solubility too low to be measured in our assay. To increase the aqueous solubility, it was proposed to add a polar solubilising side chain. The 4 and 5-position of the B-ring is pointing out of the binding site and allows for a wide range of substituents. Docking indicated that attachment of a polar group via an aniline nitrogen in the 5-position of the B-ring could be favorable as the NH might form an additional hydrogen bond with Pro933 (His84 in CDK2) of the kinase hinge. Compound **22** with an aniline in this position had improved solubility at 25 μg/mL and maintained a good JAK2 activity but unfortunately a much larger increase in CDK2 activity was also observed. Compound **23** with a basic side chain attached to the aniline was slightly less potent, with the exception of TYK2, but with the same unfavorable selectivity profile. Compound **24** with a methoxy in the 5-position of the B-ring was expected to have an unfavorable interaction with Pro933 (His84) and was therefore expected to be much less potent. However **24** was equipotent with **11** against JAK2 and much less active against CDK2. Therfore we believe that the hydrogen bond to His84 may only be formed in CDK2, as shown in Fig. 11a for **22**.

Docking indicated that a solubilising group in the 4-position of the B-ring having a basic nitrogen on a 2–3

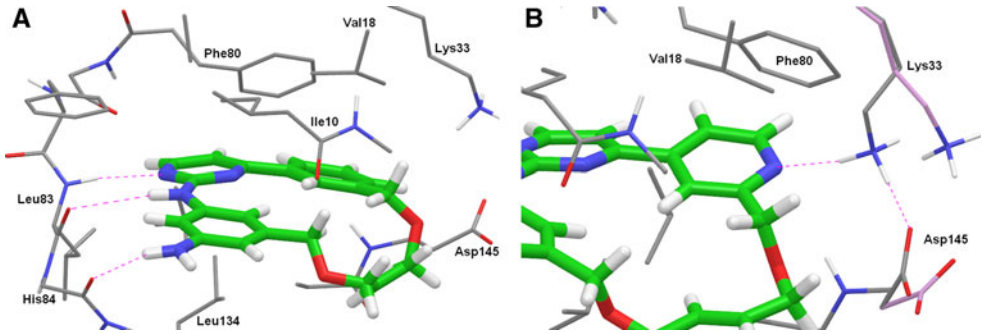


**Fig. 11** **a** Compound **22** docked into CDK2. The free aniline of **22** forms an additional hydrogen bond to the backbone carbonyl of His84 in the kinase hinge. This position may be used to attach a solubilising group, but CDK2 seems to be the only kinase for which the extra hydrogen bond is formed. **b** Compound **32** docked into CDK2. The pyridine nitrogen forms a hydrogen bond to the Lys33. The introduction of the nitrogen lowers clogP by 0.7 units, but the favorable interaction with the catalytic lysine seems only present in CDK2. The flexible sidechains of Asp145 and Lys33 was moved slightly in order for Lys33 to hydrogen bond to the inhibitor and form a salt bridge to Asp145. The original position of these sidechains is shown with *pink* carbon

atom linker attached to a phenolic oxygen may interact favorably with Asp939 (see Fig. 8). Compounds **11** and **25–27** with a pyrrolidine solubility tag proved to be very active. The C2 and C3 linkers had similar enzyme inhibitory profiles hence the C2 linker was preferred for its lower molecular weight and cLogP. However, even if the pyrrolidine basic centres did interact with Asp939, it is probably not a strong interaction as Asp939 is a surface residue. Compound **11** had a good solubility of 150 μg/mL. This was similar to the analogues **20** and **24** which also had a pyrrolidine solubility tag. In vitro and in vivo profiling of **11** proved this compound to be selective for JAK2 and FLT3, have good DMPK properties and oral efficacy in mouse models of cancer [38]. Consequently **11** (SB1518) was progressed into preclinical development.

Bulky substituents, such as morpholine and piperazine, were tolerated at the 4-position. Compounds **28–30** proved to be somewhat less potent against JAK2 than **11** but with an equally good selectivity profile. Docking indicated that the basic nitrogen in the piperazine could not form a salt bridge with Asp939. This was supported by the SAR of morpholine analogue **29**, which was found to be equipotent with the piperazine analogue **28**. At this stage in the program the medicinal chemistry team selected compound **11** as a JAK2/FLT3 preclinical development candidate, later named pacritinib, which entered the clinic in 2008. We continued investigations of the series aiming to lower the lipophilicity to increase aqueous solubility and decrease protein binding.

A-rings other than phenyl appeared to be attractive options. Introduction of one nitrogen atom into the A ring gave pyridine analogues **31–32** with cLogP values of 3.4 and 3.7, respectively. This is significantly lower than that of **11**, which has a cLogP of 4.1. As the 5 position of the A-ring is in a hydrophobic environment in all the examined kinases, **31** was expected to be less potent and decreased or

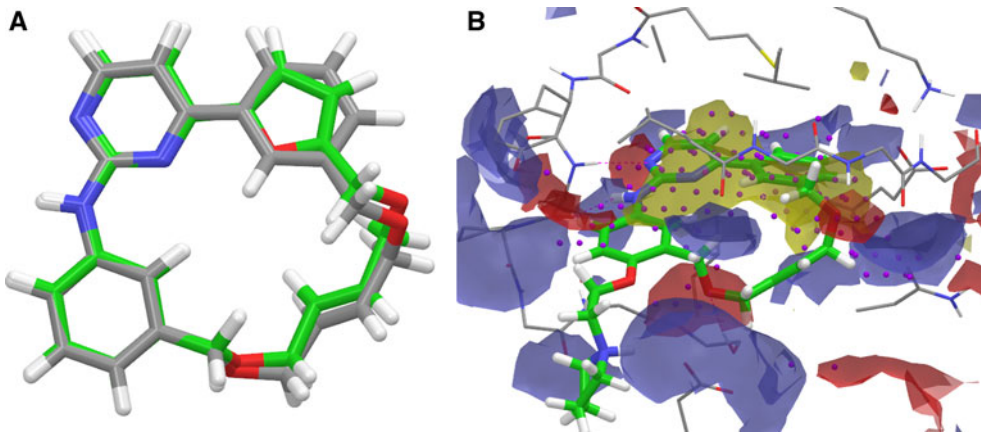


**Fig. 12** **a** The putative bioactive conformation of compound **33** (*green* carbon) superimposed on that of **11** (*grey* carbon). The side chains have been removed. **b** Sitemap [15] analysis of the JAK2 ATP-binding site with SB1518 docked. *White dots* indicate positions where it is favorable to place ligand atoms. The *yellow*, *blue* and *red grids* are hydrophobic, hydrogen bond acceptor and donor areas, respectively, of the binding site. The aromatic rings occupy a hydrophobic area while the ether oxygen falls into an acceptor area

unchanged activity was observed for all tested kinases, as compared to **11**. The 4 position is pointing towards the carboxylic acid group of the aspartate in the DFG motif and the amine of the catalytic lysine Lys33. It was hypothesized that introduction of nitrogen into this position may introduce a hydrogen bond to the aspartate (through a water molecule or, if protonated, form a salt bridge) or directly with the catalytic lysine. The $pK_a$ of the pyridine nitrogen in **32** was calculated by Epik to be 4.68. Although this value is lower than pyridine itself, it is reasonable to assume the nitrogen may be protonated when bound to a protein and in the proximity of an aspartate. However, except for a tenfold increased affinity for CDK2 the profile of **32** was similar to that of **11**. When docked into CDK2 compound **32** forms a hydrogen bond to Lys33 when the flexible side chain of this residue is moved slightly. This is shown in Fig. 11b.

A more radical change was to replace the A-ring with a 5-membered heteroaromatic ring. This changes the vector at which the macrocyclic linker branches off the biaryl, but it does not significantly change the shape of low energy conformations. This is shown in Fig. 12a where the putative bioactive conformations of **11** and **33** are superimposed. Figure 12b show a sitemap analysis of the JAK2 binding site with **11** docked. The center of the A-ring and the side pointing towards the center of the macrocyclic ring dock in a very hydrophobic environment whereas the 4, 5 and 6 positions point towards a slightly more hydrophilic environment. Compound **34**, with a thiophene A-ring, was expected to be more potent as it binds with the sulfur atom in the highly hydrophobic environment. However the clogP is only 0.1 units less lipophilic than **11**. In contrast, compound **33** (SB1578) with a furan A-ring was expected to be less potent but with a clogP of 3.7 it proved to have superior ADME properties [40] and was consequently selected for preclinical development for non-oncology indications. Compounds **35** and **36** are isomers of **33** and **34** but were less favored. Again, more lipophillic **36** is approximately fivefold more JAK2 active than the oxygen derivative **35**. The solubility of the thiophene compounds **34** and **36** was comparable to **11** while the furan analogues **33** and **36** was found to have a much improved solubility of >250 μg/mL. Compound **37** is a pyrazole analogue with the macrocyclic linker attached to a pyrazole nitrogen. Compound **37** has an improved clogP of 3.7, but it has an increased CDK2 activity. This may be due to the nitrogen acceptor of the pyrazolehydrogen bonding with Asp145 through a water molecule.

Compound **38** was designed to interact with the kinase hinge by an additional hydrogen bond as shown in Fig. 13. In **38** the C-ring is a triazole with a free amine in the 3-position. Synthesis proved challenging and the compound could only be made with a pyrimidine A-ring. With a clogP of 2.7 it is much less polar than macrocycles having the aminopyrimidine scaffold. Although the selectivity profile is good, and FLT3 potency is retained, the JAK2 activity is reduced. This is probably due to the more polar A-ring and the free amine not interacting well with the gatekeeper. It is unclear if the extra hydrogen bond is formed in JAK2 but it probably is in FLT3 to which the affinity is unchanged compared to **11** despite the more polar A-ring.

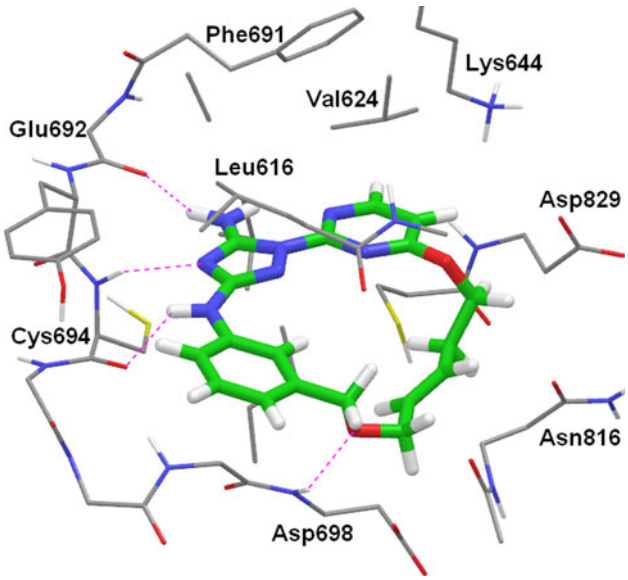


**Fig. 13** Compound **38** docked into JAK2. **38** was designed to form an extra hydrogen bond to the carbonyl oxygen of Glu692 in the backbone of the kinase hinge. However this seems only to be the case for FLT3. The affinity towards other kinases was reduced probably due to the more polar *A*-ring and reduced lipophillic interactions with the gatekeeper

## Conclusions

A screen against a kinase panel reveled that macrocycles from our Aurora project were active against other kinase targets. Subsequently these compounds became leads in our JAK2 program. Macrocycles with a basic nitrogen in the linker [14] form a salt bridge with Asp86 in CDK2 and have single digit nanomolar CDK2 potency. However, we were targeting JAK2/FLT3 selective compounds and this CDK activity was unwanted. Macrocycles with an ether linker cannot hydrogen bond to the aspartate and generally lack CDK activity. Thus we were able to obtain potent and subtype selective JAK2/FLT3 inhibitors.

The sequence identity between the JAK2 and JAK3 kinase domains is 62 % but their binding sites only differ at two residues Ser936/Cys909 and Gly993/Ala966 (JAK2/JAK3 numbering). We exploited the Ser936/Cys909 difference with

the ether oxygen in the linker which hydrogen bonds to the hydroxyl group of Ser936 of JAK2 but not Cys909 of JAK3. Thus we obtained compounds with low nanomolar JAK2 activity that were 40 fold selective over JAK3.

Our macrocycles generally have good DMPK properties and are orally efficacious in mouse models of cancer [38, 39]. Our JAK2 program was successfully completed by progressing two compounds into preclinical development. The selective JAK2/FLT3 inhibitor **11** (SB1518, Pacritinib) has now completed a phase 2 clinical trial in myelofibrosis patients and phase 2 studies for other cancers, including lymphoma, are ongoing [40]. The selective JAK2/FLT3 inhibitor **33** (SB1578) is currently in phase 1 clinical development for the non-oncology indication rheumatoid arthritis.

## References


1. Rawlings JS, Rosler KM, Harrison DA (2004) J Cell Sci 117:1281
2. Bennett M, Stroncek DF (2006) J Transl Med 4:41
3. Harpur AG, Andres AC, Ziemiecki A, Aston RR, Wilks AF (1992) Oncogene 7:1347
4. Peeters P, Raynaud SD, Cools J, Wlodarska I, Grosgeorge J, Philip P, Monpoux F, Van Rompaey L, Baens M, Van den Berghe H, Marynen P (1997) Blood 90:2535
5. Levine RL, Pardanani A, Tefferi A, Gilliland DG (2007) Nat Rev Cancer 7:673
6. Campbell PJ, Griesshammer M, Dohner K, Dohner H, Kusec R, Hasselbalch HC, Larsen TS, Pallisgaard N, Giraudier S, Le Bousse-Kerdiles MC, Desterke C, Guerton B, Dupriez B, Bordessoule D, Fenaux P, Kiladjian JJ, Viallard JF, Briere J, Harrison CN, Green AR, Reilly JT (2006) Blood 107:2098
7. Kralovics R, Teo SS, Li S, Theocharides A, Buser AS, Tichelli A, Skoda RC (2006) Blood 108:1377
8. McLornan D, Percy M, McMullin MF (2006) Ulster Med J 75:112
9. Apostolidou E, Kantarjian HM, Verstovsek S (2009) Clin Lymphoma Myeloma 9(Suppl 3):S340
10. Atallah E, Verstovsek S (2009) Expert Rev Anticancer Ther 9:663
11. Hitoshi Y, Lin N, Payan DG, Markovtsov V (2010) Int J Hematol 91:189
12. Verstovsek S (2009) Hematol Am Soc Hematol Educ Program 2009:636
13. Schafer AI (2006) Blood 107:4214
14. William AD, Lee A, Goh KC, Blanchard S, Poulsen A, Teo EL, Nagaraj H, Lee C, Wang H, Williams M, Sun ET, Hu C, Jayaraman R, Pasha MK, Ethirajulu K, Wood JM, Dymock BW (2011) J Med Chem 55:169–196
15. http://www.schrodinger.com. Schrödinger, LLC, New York (2009)
16. Chang G, Guida WC, Still WC (1989) J Am Chem Soc 111:4379
17. Jorgensen WL, Maxwell DS, Tirado-Rives J (1996) J Am Chem Soc 118:11225
18. Kaminski GA, Friesner RA, Tirado-Rives J, Jorgensen WL (2001) J Phys Chem B 105:6474
19. Hasel WH, Hendrickson TF, Still WC (1988) Tetrahedron Comput Method 1:103
20. Williams NK, Bamert RS, Patel O, Wang C, Walden PM, Wilks AF, Fantino E, Rossjohn J, Lucet IS (2009) J Mol Biol 387:219
21. Lucet IS, Fantino E, Styles M, Bamert R, Patel O, Broughton SE, Walter M, Burns CJ, Treutlein H, Wilks AF, Rossjohn J (2006) Blood 107:176
22. Boggon TJ, Li Y, Manley PW, Eck MJ (2005) Blood 106:996
23. Chrencik JE, Patny A, Leung IK, Korniski B, Emmons TL, Hall T, Weinberg RA, Gormley JA, Williams JM, Day JE, Hirsch JL, Kiefer JR, Leone JW, Fischer HD, Sommers CD, Huang HC, Jacobsen EJ, Tenbrink RE, Tomasselli AG, Benson TE (2010) J Mol Biol 400:413
24. Lawrie AM, Noble ME, Tunnah P, Brown NR, Johnson LN, Endicott JA (1997) Nat Struct Biol 4:796
25. Griffith J, Black J, Faerman C, Swenson L, Wynn M, Lu F, Lippke J, Saxena K (2004) Mol Cell 13:169
26. Berman HM, Westbrook J, Feng Z, Gilliland G, Bhat TN, Weissig H, Shindyalov IN, Bourne PE (2000) Nucleic Acids Res 28:235
27. Gasteiger E, Gattiker A, Hoogland C, Ivanyi I, Appel RD, Bairoch A (2003) Nucleic Acids Res 31:3784
28. Chenna R, Sugawara H, Koike T, Lopez R, Gibson TJ, Higgins DG, Thompson JD (2003) Nucleic Acids Res 31:3497
29. Jones DT (1999) J Mol Biol 292:195
30. Pollastri G, Przybylski D, Rost B, Baldi P (2002) Proteins 47:228
31. Still WC, Tempczyk A, Hawley RC, Hendrickson T (1990) J Am Chem Soc 112:6127
32. Bostrom J, Norrby PO, Liljefors T (1998) J Comput Aided Mol Des 12:383
33. Tannor DJ, Marten B, Murphy R, Friesner RA, Sitkoff D, Nicholls A, Honig B, Ringnalda M, Goddard WA (1994) J Am Chem Soc 116:11875
34. GraphPad. In: GraphPad Software, La Jolla (2009)
35. Bryant J, Kochanny M, Yuan S, Khim S-K, Buckman B, Arnaiz D, Bomer U, Breim H, Esperling P, Huwe C, Kuhnke J, Schafer M, Wortmann L, Kosemund D, Eckle E, Feldman R, Phillips G (2004) In: Schering Aktiengesellschaft
36. Burns CJ, Bourke DG, Andrau L, Bu X, Charman SA, Donohue AC, Fantino E, Farrugia M, Feutrill JT, Joffe M, Kling MR, Kurek M, Nero TL, Nguyen T, Palmer JT, Phillips I, Shackleford DM, Sikanyika H, Styles M, Su S, Treutlein H, Zeng J, Wilks AF (2009) Bioorg Med Chem Lett 19:5887
37. Cao JJ, Hood J, Lohse D, Mak CC, McPherson A, Noronha G, Pathak V, Renick J, Soll R, Zeng B 92007) In: Targegen, Inc
38. William AD, Lee AC, Blanchard S, Poulsen A, Teo EL, Nagaraj H, Tan E, Chen D, Williams M, Sun ET, Goh KC, Ong WC, Goh SK, Hart S, Jayaraman R, Pasha MK, Ethirajulu K, Wood JM, Dymock BW (2011) J Med Chem 54:4638
39. William AD, Lee AC, Poulsen A, Goh KC, Madan B, Hart S, Tan E, Wang H, Nagaraj H, Chen D, Lee CP, Jayaraman R, Pasha MK, Ethirajulu K, Wood JM, Dymock BW (2012) J Med Chem 55:2623–2640
40. Hart S, Goh KC, Novotny-Diermayr V, Hu CY, Hentze H, Tan YC, Madan B, Amalini C, Loh YK, Ong LC, William AD, Lee A, Poulsen A, Jayaraman R, Ong KH, Ethirajulu K, Dymock BW, Wood JW (2011) Leukemia 25:1751